Comparative analysis of intracellular and extracellular antibiotic resistance gene abundance in anaerobic membrane bioreactor effluent

Phillip Wang*, Moustapha Harb*, Ali Zarei-Baygi*, Lauren B. Stadler, and Adam L. Smith*†**

*Astani Department of Civil and Environmental Engineering, University of Southern California, 3620 S Vermont Ave, Los Angeles, CA 90089, USA

** Department of Civil and Environmental Engineering, Rice University, 6100 Main Street, Houston, TX 77005, USA

†Corresponding author (Adam L. Smith)
Phone: +1 213.740.0473
Email: smithada@usc.edu

Comparative analysis of intracellular and extracellular antibiotic resistance gene abundance in anaerobic membrane bioreactor effluent

Phillip Wang*, Moustapha Harb*, Ali Zarei-Baygi*, Lauren B. Stadler, and Adam L. Smith*†**

*Astani Department of Civil and Environmental Engineering, University of Southern California, 3620 S Vermont Ave, Los Angeles, CA 90089, USA
** Department of Civil and Environmental Engineering, Rice University, 6100 Main Street, Houston, TX 77005, USA

†Corresponding author (Adam L. Smith)
Phone: +1 213.740.0473

Abstract: The growing practice of wastewater reuse poses a significant risk to further dissemination of antibiotic resistance due to the abundance of antibiotic resistance bacteria (ARB) and antibiotic resistance genes (ARGs) in wastewater effluents. Anaerobic membrane bioreactors (AnMBRs) are an emerging wastewater treatment technology capable of reducing the total ARGs and ARB load discharged to receiving environments compared to conventional aerobic treatment processes. While size exclusion is effective at retaining ARB and its associated intracellular ARGs, the abundance and fate of extracellular ARGs in an AnMBR effluent have not been examined. This study elucidates the effect of combined antibiotics loading (ampicillin, erythromycin, and sulfamethoxazole) on the abundance of intracellular and extracellular ARGs in an AnMBR effluent over a period of five weeks. Quantification of targeted genes revealed an overall enrichment of intracellular ARGs (iARGs) and depletion of extracellular (exARGs) in response to antibiotics addition, which suggests exARG uptake as a significant mode of horizontal gene transfer in AnMBR effluents. Comparison of the iARG and exARG abundance profiles showed a potential bias for exARG uptake located on

small plasmids compared to large plasmids.

Importance: Antibiotic resistance dissemination is facilitated through horizontal gene transfer (HGT) of ARGs. Currently, conjugation is considered to be the dominant mechanism during wastewater treatment. However, recent studies have detected high abundances of exARGs , implying that transformation may play a greater role in dissemination. While previous studies quantified iARGs and exARGs in wastewater treatment facilities, they did not evaluate temporal changes between the two forms. Further, almost no research has differentiated between iARGs and exARGs in anaerobic processes, which are being considered to replace aerobic activated sludge processes. This study specifically investigates the abundance of targeted iARGs and exARGs in AnMBRs in response to antibiotic pressure to quantify potential exchange of ARGs between intracellular and extracellular compartments. Our findings suggest that exARGs located on small plasmids are preferentially taken up by cells under antibiotic pressure compared to large plasmids, which implies heterogenous HGT mechanisms among the plasmid community.

1. Introduction

The global spread of antibiotic resistance continues to be a grave threat to human health (Chioro, et al., 2015). Approximately 2 million clinical cases and 23,000 deaths related to antibiotic resistant infections occur annually in the US (Frieden, 2013). Current projections estimate that the yearly worldwide deaths related to antibiotic resistance will reach 10 million by the year 2050 (O'Neil, 2014). While conventional wastewater treatment plants (WWTPs) are effective at managing organics and nutrients, they are not designed or operated to treat emerging contaminants like antibiotic resistance genes (ARGs) and antibiotic resistant bacteria (ARB). With growing awareness of antibiotic resistance, numerous studies have identified WWTPs as hot spots for the propagation of ARGs and ARB (Bouki, et al., 2013, Michael, et al., 2013). Studies on the effluent quality of conventional WWTPs have reported incomplete removal of both ARGs and ARB (McConnell, et al., 2018, Quach-Cu, et al., 2018). Therefore, ARGs and ARB in treated wastewater can continue to proliferate via horizontal gene transfer (HGT) and vertical gene transfer when discharged into receiving environments.

Analyses of sediment microbial communities near outfall sites of WWTPs have detected similar patterns of ARGs and gene classes as those in WWTP effluents (Chu, et al., 2018). While the influence of effluent ARGs on the sediment microbial community is less prominent with increasing distance from effluent outfall sites, the practice of water reuse (e.g., for agricultural irrigation), removes the environmental buffers associated with conventional handling of treated wastewater and results in direct ARGs and ARB loading to receiving soils. Observations of recent studies generally suggest a positive association

between proliferation of soil ARGs and contact time with treated wastewater (Fahrenfeld, et al., 2013, Han, et al., 2016, Corno, et al., 2019). Therefore, reducing the abundance of antibiotic resistance elements in treated wastewater is critical to limiting the spread of antibiotic resistance in water reuse applications (Pruden, et al., 2013).

Anaerobic membrane bioreactors (AnMBRs) are an emerging wastewater treatment technology that couples anaerobic biological treatment with membrane separation to recover energy, reduce sludge production, and produce a high-quality effluent comparable to activated sludge processes (Smith, et al., 2012). Although low in carbon, AnMBR effluents are rich in nutrients and can be utilized effectively in agricultural reuse scenarios to offset artificial fertilizer needs. Further, the combination of membrane separation with slower microbial growth under anaerobic conditions can theoretically reduce the load of ARGs and ARB in treated wastewater (Le, et al., 2018). However, the fate of ARGs and ARB within AnMBRs remains poorly understood. Previously, we reported the first long-term investigation of eight ARGs, spanning multiple ARG subtypes, in a bench-scale AnMBR under step-wise increases in influent antibiotic concentrations (Zarei-Baygi, et al., 2019). Our results revealed stark differences in the ARG abundance profile of the biomass versus effluent under all conditions tested. The steep reduction in the ARG abundance profile from the biomass to the effluent is likely due to the effective microbial retention by the submerged membranes(Li, et al., 2019). However, size exclusion by membrane pores may not retain extracellular ARGs (exARGs). Moreover, a growing number of studies have reported a high abundance of extracellular DNA (exDNA) in WWTPs and have suggested that the transformation of exARGs might play a larger role in antibiotic resistance dissemination than previously considered (Mao, et al., 2014,

89 Dong, et al., 2019). Therefore, we suspect that the ARG profile in AnMBR effluent may
90 be heavily influenced by exARGs passing through the membrane pores.

91 Of concern to human health are the many human pathogens known to enter
92 natural competency (e.g., *Campylobacter*, *Haemophilus*, *Helicobacter*, *Neisseria*,
93 *Pseudomonas*, *Staphylococcus*, *Streptococcus*, *Vibrio*), with some pathogenic strains
94 having a subset of their clonal population in a state of constitutive competency (e.g.,
95 *Neisseria gonorrhea* and *Helicobacter pylori).* While the transformation of exDNA may be
96 limited to smaller plasmids and not be effective at disseminating large multi-drug resistant
97 plasmids, smaller non-conjugative plasmids can also confer multi-drug resistance in
98 bacteria (San Millan, et al., 2009, Lean and Yeo, 2017). Therefore, the direct loading of
99 exARGs, iARGs, and ARB to areas of potential human contact could significantly
100 accelerate the development of antibiotic resistant human pathogens.

101 Previous studies on exARGs and iARGs have focused on investigating their
102 abundance at multiple environmental locations, such as various types of WWTPs, water
103 sources, and sediments (Mao, et al., 2014, Wang, et al., 2016, Zhang, et al., 2018, Dong,
104 et al., 2019). However, no studies to date have examined the effect of antibiotics addition
105 on exARG and iARG abundance over time. The dynamic relationship between exARGs
106 and iARGs within a microbial community in antibiotic-influenced environments remains
107 an area of much needed investigation. The potential cyclical movement of exDNA
108 between microbial hosts and the extracellular compartment may be a fundamental
109 mechanism for the conservation and propagation of ARGs and ARG associated MGEs
110 between distinct and distant microbial communities. While AnMBRs could theoretically

lessen the load of ARGs and ARB to receiving environments compared to conventional treatment process, the potential propagation of exARGs in the effluent stream needs further research. In this study, we characterized the effect of a combined mixture of antibiotics loading on the antibiotic resistance characteristics of an AnMBR effluent stream.

2. Materials and Methods

2.1 AnMBR Configuration and Monitoring

A bench-scale AnMBR with a working volume of 5 L was operated at 25 °C as previously described (Zarei-Baygi, et al., 2019). Briefly, the AnMBR housed three separate submerged flat-sheet silicon carbide microfiltration membranes (0.1 μm pore size, Cembrane, Denmark), with a total effective membrane area of approximately 0.015 m^2. Synthetic wastewater was used to reduce the variable background influence of antibiotics, ARB, and ARGs associated with real wastewater. The synthetic wastewater recipe was formulated to represent US domestic wastewater (Supporting Information (SI) Table S1) (Smith, et al., 2013).The AnMBR was seeded with sludge from a mesophilic anaerobic digester at the Joint Water Pollution Control Plant (Carson, CA). AnMBR performance was monitored by measuring water quality parameters including soluble chemical oxygen demand (sCOD), total chemical oxygen demand (tCOD), volatile fatty acids (VFAs), and mixed liquor and volatile suspended solids (MLSS/MLVSS). Biogas production was monitored by an in-line gas flowmeter and assessed for methane content by gas chromatography with flame ionization detection (GC-FID). Steady AnMBR performance was defined as low effluent COD (<50 mg/L), stable biogas production, and

high methane content (>60%) over a phase of 10 days. After reaching steady AnMBR performance, three antibiotics, sulfamethoxazole (sulfonamide), erythromycin (macrolide), and ampicillin (β- lactam), were added to the influent at 250 µg/L (day 3) to represent antibiotic concentrations at the high range of hospital wastewater(Xu, et al., 2016, Kulkarni, et al., 2017). Influent antibiotics concentration was maintained at 250 µg/L for the entirety of the antibiotics loading phase (day 3 to day 35). Effluent lines were cleaned with sodium hypochlorite 0.5% (v/v) before the start of the experiment. Membrane modules were removed for physical and chemical cleaning 0.5% (v/v) before the addition of antibiotics.

2.2 Antibiotic Quantification

Antibiotic quantification procedures were carried out as previously described (Zarei-Baygi, et al., 2019). Briefly, individual antibiotic concentrations of each sample were analyzed by direct injection liquid chromatography mass spectrometry with electrospray ionization (LC-ESI-MS) on a 6560 Ion Mobility Quadrupole Time-of-Flight (IM-QTOF) LC-MS system (Agilent). Chromatographic separation and ionization were achieved by employing a 1290 Infinity UHPLC with EclipsePlus C18 column (2.1 mm; 50 mm; 1.8um) followed by a Dual Agilent Jet Stream (ASJ) ESI. Standard curves were generated by matrix-matched external calibration of serial dilutions of antibiotics purchased from Sigma (>99% purity). Practical quantitation limits (PQL) for each target compound were determined to be <0.1 µg/L based on previously optimized LC-ESI-MS conditions (Zarei-Baygi, et al., 2019). Details on sample preparation, optimized LC program, and MS operational conditions can be found in the (SI Table 3).

2.3 qPCR quantification of ARGs

qPCR reactions were carried out using a LightCycler 96 (Roche, Basel, Switzerland) targeting a set of nine genes. The nine targeted genes included: a class one integrase gene (*intI*1), a single copy per cell gene (*rpo*B), and seven ARGs conferring resistance to β-lactams (*oxa*-1 and *amp*C), macrolides (*erm*F), sulfonamides (*sul1* and *sul2*), and tetracyclines (*tet*W and *tet*O). Targeted ARGs were chosen based on their common detection in domestic wastewater studies (Pruden, et al., 2006, Ma, et al., 2011, Munir, et al., 2011). qPCR reactions were done in 20 µL reactions with 10 µL of qPCR master mix (Forget-Me-Not EvaGreen, Biotium, Fermont, CA), forward and reverse primers at 0.25 µM (final concentration) each, 1 µL of DNA template, and ddiH_2O. Each reaction was performed in triplicate. Details for the thermal cycling conditions for all targeted ARGs are provided in the (SI Table 2). All qPCR results were normalized to effluent sample volume for comparison of ARG abundance across sampling points. Results were represented as total abundance instead of normalized values relative to chromosomal *rpoB* gene due to previous reports of faster decay rates for chromosomal DNA versus plasmid DNA, which could lead to inflated reports of exARG concentration when normalizing to chromosomal genetic markers (Mao, et al., 2014).

2.4 Intracellular and extracellular DNA extraction

iDNA and exDNA extractions were carried out using the same 500 mL effluent samples for each sampling point. Internal standards to correct for DNA recovery across sample processing were added to each effluent sample by spiking with approximately $2x10^6$ copies of plasmid pUC19 immediately after collection. Spiked effluent samples

were filtered using vacuum filtration through sterile cellulose acetate membrane filters (0.22um, 45mm diameter, Whatman). Processed filters with collected biomass were used for iDNA extractions. The processed filters were cut into pieces and placed in 2 mL sterile tubes and mixed with lysis buffer before bead beating with zirconium beads. iDNA extractions were carried out using the Maxwell 16 instrument (Promega) and eluted in 100µl of buffer AE. The filtrates were used for exDNA extractions using nucleic acid adsorption particles (NAAP) adapted from Wang et al (Wang, et al., 2016). Briefly, autoclaved $Al(OH)_3$ solutions (47.8%, V/V) were mixed with 5% (g/mL) silica gel (60-100 mesh size, Sigma) and dried for 36 hours at 60°C. Dried silica gels coated with $Al(OH)_3$ were then sealed in a cylindrical glass container (1.5 x 40 cm) as NAAP columns. The previously mentioned filtrate samples were passed through the NAAP columns. Adsorbed exDNA were eluted from the NAAP columns with 100 mL of elution buffer (15 g/L NaCl, 30 g/L tryptone, 15 g/L beef extract, 3.75 g/L glycine, 0.28 g/L NaOH, pH of 9.3 ± 0.2). Eluates were then collected and filtered with polyethersulfone filters (0.22 um, Millipore, USA). ExDNA in the filtrates were precipitated using an equal volume of isopropanol, incubated at room temperature for 16 h, and centrifuged at 10,000g for 10 min at room temperature. After decantation of the supernatant, the centrifuged pellets were mixed with 70% ethanol (v/v) and centrifuged again at 10,000 g for 5 min at room temperature. After a second decantation, the residual ethanol was evaporated in a 60 °C oven and the pellets were re-suspended in 4 mL of sterilized TE buffer. Extracted DNA samples were quantified using Quant-iT PicoGreen (Thermo Fisher) and a BioSpectrometer (Eppendorf, Hamburg, Germany). iDNA extraction efficiency was carried out without the use of an iDNA internal standard due to the consistent performance of the Maxwell 16

instrument (Promega) (data not shown). Extraction efficiency of each exDNA extraction was assessed using spiked pUC19 serving as the exDNA standard (SI Table 2). The qPCR results for each exARG data point were adjusted based on the corresponding extraction efficiency of the exDNA standard (e.g,, gene copies of exampC/(gene copies of pUC19/total spiked gene copies of pUC19)). All DNA extracts were stored at -80 °C until analysis.

2.5 Statistical Analysis Methods

Statistical analyses were performed using MaxStat Lite 3.6. Significant changes in ARG abundance at different time points were assessed using a 2-tailed unpaired student's t-test. Pearson and Spearman rank correlations were used to assess correlations between data points over a 95% confidence interval. Strength of correlations were identified based on the Pearson coefficient r, as $r > 0.7$ or $r < -0.7$ for strong correlations, $-0.7 < r < -0.5$ or $0.5 < r < 0.7$ for moderate correlations, and $-0.5 < r < -0.3$ or $0.3 < r < 0.5$ for weak correlations. Pearson correlations were performed on separated iARG and exARG data sets. Spearman rank correlations were performed on the combined iARG and exARG data sets due to the dynamic nature of gene transport, synthesis, and degradation.

2.6 Heterotrophic Plate Counts

Total bacteria and ARB in the effluent were enumerated using the heterotrophic plate count method with nutrient agar as the media (Federation, 2005). Ampicillin (AMP), tetracycline (TET), erythromycin (ERY), and sulfamethoxazole (SMX) resistant bacteria

221 counts were determined by growth on nutrient agar plates supplemented with
222 corresponding AMP, TET, SMX, or ERY. TET resistance bacteria counts were included
223 as a control given the lack of tetracycline in the synthetic wastewater. Final concentration
224 for each antibiotic was guided by MIC reports in previous studies: AMP, 16 μg/mL; TET,
225 16 μg/mL; ERY, 50.4 μg/mL; and SMX, 18.1 μg/mL(Pei, et al., 2006, Zheng, et al., 2017).
226 All plates were incubated at 35°C for 48 hrs.

227 ## *3. Results and Discussion*

228 ### *3.1 Stable Reactor Performance Under Mixed Antibiotics Loading*

229 Effluent COD averaged 45.4 ± 10.7 mg/L, equating to a COD removal of 90.0 ±
230 1.8% throughout the experimental phase. Average biogas production and methane
231 content were 736 ± 20 mL/d and 536 ± 14 mL/d, respectively. The average MLSS and
232 MLVSS were 10.6 g/L ± 1.3 and 9.6 ± 0.3 g/L, respectively. The addition of mixed
233 antibiotics (SMX, ERY, and AMP), at 250 ug/L each, to the influent showed minimal
234 perturbation to the reactor performance (SI Fig1), except for day 17 which saw a slight
235 decrease in biogas production. These results are consistent with previous studies which
236 have shown that this range of antibiotic loading on anaerobic reactors is well below the
237 threshold that would cause a disruption in system performance (Aydin, et al., 2015, Xiong,
238 et al., 2017). Antibiotic removal was relatively stable across the operational phase, with
239 AMP removal ranging from 89-98%, followed by SMX at 69-78%, and ERY at 40-58%
240 (Fig 1). The wide-ranging specific removal rates of these antibiotics in the AnMBR are
241 consistent with those observed for other mainstream anaerobic wastewater treatment

242 systems, which can vary greatly in comparison to conventional aerobic treatment
243 schemes (Harb, et al., 2019).

244 *3.2 SMX Resistant Bacteria Count Approaches Total Culturable Bacteria Count*

245 Overall, SMX resistance showed the greatest degree of proliferation among the
246 types of antibiotic resistance tested. SMX resistant bacteria in the effluent increased by >
247 3 log (CFU/mL) ($p=0.032$) over the course of the experiment, with the number of total
248 bacteria increasing by 0.68 log (CFU/mL) ($p=0.027$) over the same duration (Fig 2). The
249 ratio of SMX resistant bacteria to total bacteria exhibited a non-linear rise from 55.5%
250 (day 1) to 96.5% (day 57). In comparison, the ratio of AMP resistant bacteria to total
251 bacteria rose from 68.7% to 75.4% and the ratio of ERY resistant bacteria to total bacteria
252 fell from 89.3% to 76.7%. As expected, (given no addition of TET in the influent) counts
253 for TET resistant bacteria frequently fell below the limit of detection (LOD= 10 CFU/mL).
254 Among the ARB types tested, only SMX resistant bacteria showed a positive association
255 between the increase in effluent abundance and antibiotic dosing. Our findings were
256 consistent with our previous report and Le et al., where sulfamethoxazole was found to
257 be one of three antibiotics to increase with its corresponding ARB among 19 targeted
258 antibiotics in an MBR system (Le, et al., 2018, Zarei-Baygi, et al., 2019). It is important to
259 note that heterotrophic plate counts only capture a small fraction of microbial diversity.
260 Further, aerobic plating of effluents from anaerobic systems favors quantification of
261 facultative microorganisms and excludes detection of obligate anaerobes. Despite these
262 methodological limitations, HPC used in this capacity still provides useful data regarding

263 relative changes in ARB, which complements our parallel use of culture-independent
264 methods (i.e., qPCR).
265
266 *3.3 Total iARGs and exARGs Showed Varied Response Towards Antibiotics*
267 *Addition*

268 Total iARGs were consistently more abundant than total exARGs by at least 2 log
269 (Gene Copies/mL) throughout the experimental period (Fig 3). Similar findings of higher
270 iARG versus exARG abundance have been reported in most aquatic environments
271 examined (Nielsen, et al., 2007, Mao, et al., 2014, Zhang, et al., 2018, Hao, et al., 2019).
272 In contrast, studies on sediment samples frequently report higher abundance of exARGs
273 than iARGs (Mao, et al., 2014, Dong, et al., 2019). The higher abundance of exARGs
274 versus iARGs in sediment samples is likely due to the adsorption of exDNA to soil colloids,
275 clay particles, and organic matter that can decrease the susceptibility of exDNA
276 degradation from nuclease attacks (Crecchio and Stotzky, 1998, Demanèche, et al.,
277 2001).

278 The addition of antibiotics in the influent coincided with increasing abundance of
279 total iARGs in AnMBR effluent, rising from 5.52 (day 1) to 7.13 (day 35) log (Gene
280 Copies/ml). The observed increase in total iARGs during the antibiotics loading phase is
281 likely due to the selection for ARB and their associated ARGs in the effluent stream. The
282 abundance of total exARGs, over the same time frame, exhibited a non-linear decrease
283 from 3.46 (day 1) to 3.16 (day 35). Interestingly, total exARGs showed an initial rise to
284 4.2 log (gene copeies/mL) (day 21) followed by a precipitous drop to 2.11 log (Gene

Copies/ml) midway through the experimental run (day 28). The initial increase in total exARGs before day 28 could be due to antibiotic induced exDNA release for the purpose of biofilm formation and HGT (Zafra, et al., 2012, Okshevsky and Meyer, 2015, Sugimoto, et al., 2018). Moreover, antibiotics, biofilm formation, and exDNA are all associated with the induction of natural competency of many bacterial species (Li, et al., 2001, Ibanez de Aldecoa, et al., 2017). Therefore, an increase in competent microbial members within the effluent stream could explain the sharp decrease in total exARGs abundance on day 28. In the post-antibiotics loading phase, the increase in total exARGs is likely due to the loss of ARG-associated MGEs as the fitness advantage of retaining ARG-associated MGEs decreases. However, the persistence of MGEs in microbial hosts under antibiotic-free conditions is influenced by the surrounding genes. While low copy large plasmids typically encode for additional maintenance genes (e.g., partitioning and toxin-antitoxin systems) that promote their own survival in the absence of antibiotic pressure (Ghaly and Gillings, 2018), high copy small plasmids do not encode for these maintenance genes and are generally more easily lost in the absence of strong selective pressure.

3.4 Mixed-Antibiotics Loading Increases the Abundance of Effluent iARGs

In the pre-antibiotics phase, *intI*1 was the most abundant target gene detected in the effluent, followed by *sul*1, *rpoB*, *sul*2, *tet*O, *tet*W, *erm*F, *oxa*-1, and *amp*C (Fig 4). During the antibiotics loading phase, the abundance of *sul*2 exhibited the highest increase, rising from 4.57 to 7.08 log (Gene Copies/ml) ($p<0.01$). The abundance of s*ul*1 and *intI*1 increased from 5.9 to 6.56 log (Gene Copies/ml) ($p=0.168$) and from 5.46 to 6.21 log (Gene Copies/ml) ($p=0.238$), respectively. The relatively high abundance of *sul*1, *sul*2,

and *intI*1 among targeted ARGs in our study is consistent with previous reports (Rowe, et al., 2016, Xu, et al., 2016, Zarei-Baygi, et al., 2019). Interestingly, the abundance of *oxa*-1 rose from 2.39 to 3.58 log (Gene Copies/ml) ($p < 0.01$), while the abundance of *amp*C decreased from 1.16 to 0.9 log (Gene Copies/ml) ($p=0.02$). The preferential selection of *oxa*-1 over *amp*C could be due to the co-localization of *oxa*-1 and *sul*2 on the same MGE, which would allow for the co-selection of *oxa*-1 from the SMX addition. This hypothesis is supported by the strong correlation between *sul*2 and *oxa*-1 ($r= 0.772$) ($p<0.01$) and the low AMP (2.8 µg/L to 22.45 µg/L) selective pressure in the effluent. Despite high ERY concentrations (107.0 µg/L to 130.5 µg/L) in the effluent, *erm*F abundance showed modest increase from 2.91 to 3.86 log (Gene Copies/ml) ($p<0.01$).

In the post-antibiotics phase, *sul*2 levels significantly dropped by 2.16 log (Gene Copies/ml) ($p<0.01$). Consistent with our previous co-localization hypothesis, the abundance of *oxa*-1 showed a similar sharp decrease, dropping from 3.5 to 2.08 log (Gene Copies/ml) ($p<0.01$). Additional iARG decreases included *erm*F, *tet*O, and *tet*W, which declined in abundance from 3.68 to 2.72 log (Gene Copies/ml) ($p <0.01$), 3.27 to 2.31 log (Gene Copies/ml) ($p <0.01$), and 3.67 to 2.86 log (Gene Copies/ml) ($p <0.01$), respectively. Surprisingly, the abundance of *sul*1 and *intI*1 remained elevated at 6.59 and 7.19 log (Gene Copies/ml), respectively. The elevated concentrations of *sul*1 and *intI*1 genes in the post antibiotics phase may be due to the greater persistence of low copy number large plasmids compared to high copy small plasmids in microbial hosts (Carroll and Wong, 2018). On a population level, non-conjugative plasmids tend to be smaller in size and are present in higher copy numbers (up to 200 copies per cell) compared to conjugative plasmids, which tend to be much larger in size and present in lower copy

numbers (<10 copies per cell) (Watve, et al., 2010, Shintani, et al., 2015). Under selective pressure, high copy number plasmids could theoretically increase in abundance within a microbial community more rapidly than low copy plasmids. However, small non-conjugative plasmids typically do not encode for maintenance or stability genes and are easily lost when the selective pressure is removed. In contrast, low copy conjugative plasmids may exhibit longer persistence within a microbial community due to additional maintenance systems encoded on the plasmid backbone (e.g., partitioning and toxi-antitoxin systems) (Garcillan-Barcia, et al., 2011). Overall, *sul*1 and *sul*2 were the two most abundant ARGs detected and *sul*2 exhibited the greatest increase under antibiotic pressure. Further, the sharp rise of *sul*2 in response to antibiotic stress and the persistence *of sul*1 in the post-antibiotics phase is consistent with the SMX resistant bacteria proliferation observed in our HPC results.

Pearson correlation analysis of the iARG data set revealed significant correlations between two sets of genes, *sul*2, *oxa*-1, and *tet*O ($r>0.65$, $p<0.05$) and *erm*F, *sul*1, and *intI*1 ($r > 0.6$, $p <0.05$), which suggests the presence of multi-drug resistant plasmids and/or distinct modes of plasmid propagation rates (e.g., low versus high copy plasmid). Moreover, *sul*1 was strongly correlated with *intI1* ($r = 0.869$, $p < 0.01$), while no correlation was found between *sul*2 and *intI*1 ($r = -0.059$, $p =0.853$), which suggests that the discrepant response of *sul*1 and *sul*2 to the addition of antibiotics was attributed to the different types of MGEs surrounding *sul*1 and *sul*2. Consistent with this explanation, previous studies examining the characteristics of isolated plasmids harboring *sul*1 and *sul*2 commonly detected *sul*2 on small non-conjugative plasmids whereas *sul*1 was exclusively found on large conjugative plasmids (Enne, et al., 2004, Antunes, et al., 2005,

353 San Millan, et al., 2009, Wu, et al., 2010, Dominguez, et al., 2019). The strong correlation
354 between *erm*F with *sul*1 and *intI*1 suggest that *erm*F is either co-localized with *sul*1 and
355 *intI*1 or located on similar low copy number conjugative plasmids, which could explain the
356 modest increase in abundance for *sul*1, *int*1, and *erm*F despite significant concentrations
357 of SMX (54.9 µg/L to 75.2 µg/L) and ERY (107.0 µg/L to 130.5 µg/L) in the effluent stream.

358 *3.5 Temporal Abundance Prolife of Effluent exARGs and iARGs Revealed*
359 *Distinct Patterns*

360 In the pre-antibiotics phase, all exARGs were detected, ranging from 0.25 to 3.1
361 log (Gene Copies/ml) (Fig 5). Interestingly, the addition of antibiotics coincided with an
362 overall decrease in exARG abundance, which contrasted the enrichment of iARGs during
363 the same period. Similar to iARGs, exARGs are likely associated with MGEs of varied
364 sizes. The uptake of exDNA by microbial hosts has been documented to favor small
365 plasmids and DNA fragments, which could cause the overall variability of exARG
366 abundance (Prudhomme, et al., 2006, Slager, et al., 2014). Therefore, the size of the
367 genetic carrier harboring exARG would influence its rate of degradation and uptake by
368 microbial hosts.

369 Pearson correlation analysis of the exARG data set revealed distinct patterns of
370 removal, which supports the hypothesis of size dependent exDNA uptake. Similar to the
371 Pearson correlation analysis for iARGs, extracellular *sul*1 was strongly correlated with
372 extracellular *intI*1 ($r= 0.87$, $p<0.01$). Interestingly, extracellular *sul*2 was strongly
373 correlated with extracellular *intI*1 as well ($r=0.78$ $p<0.01$) and was moderately correlated
374 with extracellular *sul*1 ($r=.59$ $p<0.01$). While some studies have identified *sul*2 to be

375 distinctly separate from *sul*1 and *intI*1, a few reports have detected *sul*2 genes on large
376 conjugative plasmids along with *sul*1 and *intI*1 genes (Phuong Hoa, et al., 2008, Wu, et
377 al., 2010, Wu, et al., 2010). The positive correlation of extracellular *sul*1, *sul*2, and *intI*1 in
378 the extracellular compartment could be due to the lower uptake efficiency of large
379 plasmids compared to small plasmids. Since *sul*2 has been documented on both large
380 and small plasmids, there could be a preferential uptake of small *sul*2-associated
381 plasmids while leaving behind larger *sul*2-associated plasmids. From the iARG profile,
382 intracellular *erm*F, *sul*1, and *intI*1 all exhibited propagation patterns resembling those of
383 low copy number conjugative plasmids, which are generally larger than non-conjugative
384 plasmids (Garcillan-Barcia, et al., 2011). Since exARGs are simply the cell-free form of
385 iARGs, the greater persistence of extracellular *erm*F, *sul*1 and *intI*1 over extracellular *sul*2,
386 *oxa*-1, and *tet*O could be due to the lower uptake efficiency of larger plasmids compared
387 to smaller plasmids.

388 Spearman rank correlation analysis was performed on the combined iARG and
389 exARG data sets to further asses the temporal relationship between iARGs and exARGs.
390 Among the ARGs examined, only extracellular *sul*2 and extracellular *tet*W were negatively
391 correlated to intracellular *sul*2 ($r=-0.68$, $p<0.01$) and intracellular *tet*W ($r = -0.836$, p
392 <0.01), respectively. The negative correlation between extracellular *sul*2 and intracellular
393 *sul*2 is consistent with our hypothesis that exARGs can be taken up and enriched within
394 microbial hosts. The lack of a significant correlation among the remaining exARGs and
395 their intracellular counterpart could be due to additional barriers involved in acquiring and
396 maintaining exogenous genes. As stated previously, the uptake of exDNA by microbial
397 hosts would likely favor small plasmids and DNA fragments Further, the maintenance of

398 exogenous genes, including ARGs, on linear DNA fragments would require recirculation
399 or integration into the microbial host genome through homologous recombination or
400 transposable elements. In general, non-integrated or circularized fragments would likely
401 be degraded for metabolic purposes or released back into the environment. Therefore,
402 the uptake of exDNA could be the first step in acquiring new functional traits and the
403 quality and compatibility of the genetic carrier adds further selection to the maintenance
404 of the acquired genes. Our findings add support to the hypothesis that the extracellular
405 compartment within microbial communities can serve as a reservoir for genetic resources,
406 including ARGs, with potential uptake biases toward small plasmids or DNA fragments.

407 While *in vitro* studies attempting to induce natural competency for many bacterial
408 species have shown limited success, the complexities of environmental conditions are
409 difficult to recreate in controlled laboratory conditions. Further, the induction of natural
410 competency for some bacterial strains have been shown to rely on the production of
411 signaling molecules from other bacterial species (Zhu, et al., 2011). In the context of
412 wastewater reuse, treated wastewater could provide high concentrations of exARGs,
413 environmental stressors, and signaling molecules from highly complex microbial
414 communities that could promote a feedback loop for exDNA release, biofilm formation,
415 and natural competency in the receiving microbial community. This cyclical uptake and
416 release of exARGs, particularly in plasmid form, could increase the total abundance of
417 exARGs within the extracellular matrix due to multiple replication cycles of plasmids within
418 microbial hosts. Additional studies are needed to unravel the complex dynamics between
419 exARG uptake and release within receiving environments such as soil microbial
420 communities.

In this study, we have shown that under mixed-antibiotics loading (SMX, ERY, and AMP at 250 µg/L), SMX resistant bacteria increase from 55.5% to 96.5% of total culturable bacteria in the effluent. Complimentary qPCR analysis of iARG abundance revealed a stark increase in *sul*2 and the persistence of *sul*1 abundance, which is consistent with our observation of the dominance of SMX resistant bacteria in HPC results. Finally, qPCR analysis of the exARG abundance over the same duration revealed an inverse trend for most exARGs and their intracellular counterparts. Most notably, extracellular *sul*2 was negatively correlated to intracellular *sul*2 ($r = -0.68$, $p = 0.001$), which suggests that competent cells can acquire antibiotic resistance from exARGs. However, it is important to note that qPCR assays are limited to the quantification of pre-determined genes. Further, the correlations drawn in this paper would benefit from experiments directly tracking the movements of iARGs and exARGs. Future studies should use metagenomic guided qPCR analysis to analyze ARGs pertinent to their research question(s) along with their associated MGEs.

References

Antunes, P., Machado, J., Sousa, J.C., and Peixe, L. (2005) Dissemination of sulfonamide resistance genes (sul1, sul2, and sul3) in Portuguese Salmonella enterica strains and relation with integrons, *Antimicrob Agents Chemother* **49**: 836-839.

Aydin, S., Ince, B., Cetecioglu, Z., Arikan, O., Ozbayram, E.G., Shahi, A., and Ince, O. (2015) Combined effect of erythromycin, tetracycline and sulfamethoxazole on performance of anaerobic sequencing batch reactors, *Bioresource technology* **186**: 207-214.

Bouki, C., Venieri, D., and Diamadopoulos, E. (2013) Detection and fate of antibiotic resistant bacteria in wastewater treatment plants: a review, *Ecotoxicol Environ Saf* **91**: 1-9.

Carroll, A.C., and Wong, A. (2018) Plasmid persistence: costs, benefits, and the plasmid paradox, *Canadian Journal of Microbiology* **64**: 293-304.

Chen, S., and Smith, A.L. (2018) Methane-driven microbial fuel cells recover energy and mitigate dissolved methane emissions from anaerobic effluents, *Environmental Science: Water Research & Technology* **4**: 67-79.

Chioro, A., Coll-Seck, A.M., Hoie, B., Moeloek, N., Motsoaledi, A., Rajatanavin, R., and Touraine, M. (2015) Antimicrobial resistance: a priority for global health action, *Bull World Health Organ* **93**: 439.

Chu, B.T.T., Petrovich, M.L., Chaudhary, A., Wright, D., Murphy, B., Wells, G., and Poretsky, R. (2018) Metagenomics Reveals the Impact of Wastewater Treatment Plants on the Dispersal of Microorganisms and Genes in Aquatic Sediments, *Applied and Environmental Microbiology* **84**: e02168-02117.

Corno, G., Yang, Y., Eckert, E.M., Fontaneto, D., Fiorentino, A., Galafassi, S., et al. (2019) Effluents of wastewater treatment plants promote the rapid stabilization of the antibiotic resistome in receiving freshwater bodies, *Water Res* **158**: 72-81.

Crecchio, C., and Stotzky, G. (1998) Binding of DNA on humic acids: Effect on transformation of Bacillus subtilis and resistance to DNase, *Soil Biology and Biochemistry* **30**: 1061-1067.

Demanèche, S., Jocteur-Monrozier, L., Quiquampoix, H., and Simonet, P. (2001) Evaluation of biological and physical protection against nuclease degradation of clay-bound plasmid DNA, *Applied and environmental microbiology* **67**: 293-299.

Dominguez, M., Miranda, C.D., Fuentes, O., de la Fuente, M., Godoy, F.A., Bello-Toledo, H., and Gonzalez-Rocha, G. (2019) Occurrence of Transferable Integrons and sul and dfr Genes Among Sulfonamide-and/or Trimethoprim-Resistant Bacteria Isolated From Chilean Salmonid Farms, *Front Microbiol* **10**: 748.

Dong, P., Wang, H., Fang, T., Wang, Y., and Ye, Q. (2019) Assessment of extracellular antibiotic resistance genes (eARGs) in typical environmental samples and the transforming ability of eARG, *Environment International* **125**: 90-96.

Enne, V., M Bennett, P., Livermore, D., and Hall, L. (2004) *Enhancement of host fitness by the sul2-coding plasmid p9123 in the absence of selective pressure*, 958-963.

Fahrenfeld, N., Ma, Y., O'Brien, M., and Pruden, A. (2013) Reclaimed water as a reservoir of antibiotic resistance genes: distribution system and irrigation implications, *Front Microbiol* **4**: 130.

Federation, W.E.a.A. (2005) Standard methods for the examination of water and wastewater, *APHA*.

Frieden, T. (2013) Antibiotic Resistance Threats in the United States, 2013, *Brochure - US Centrs for Disease Control and Prevention*.

Garcillan-Barcia, M.P., Alvarado, A., and de la Cruz, F. (2011) Identification of bacterial plasmids based on mobility and plasmid population biology, *FEMS Microbiol Rev* **35**: 936-956.

Ghaly, T.M., and Gillings, M.R. (2018) Mobile DNAs as Ecologically and Evolutionarily Independent Units of Life.

Han, X.M., Hu, H.W., Shi, X.Z., Wang, J.T., Han, L.L., Chen, D., and He, J.Z. (2016) Impacts of reclaimed water irrigation on soil antibiotic resistome in urban parks of Victoria, Australia, *Environ Pollut* **211**: 48-57.

Hao, H., Shi, D.-y., Yang, D., Yang, Z.-w., Qiu, Z.-g., Liu, W.-l., et al. (2019) Profiling of intracellular and extracellular antibiotic resistance genes in tap water, *Journal of Hazardous Materials* **365**: 340-345.

Harb, M., Lou, E., Smith, A.L., and Stadler, L.B. (2019) Perspectives on the fate of micropollutants in mainstream anaerobic wastewater treatment, *Curr Opin Biotechnol* **57**: 94-100.

Ibanez de Aldecoa, A.L., Zafra, O., and Gonzalez-Pastor, J.E. (2017) Mechanisms and Regulation of Extracellular DNA Release and Its Biological Roles in Microbial Communities, *Front Microbiol* **8**: 1390.

Kulkarni, P., Olson, N.D., Raspanti, G.A., Rosenberg Goldstein, R.E., Gibbs, S.G., Sapkota, A., and Sapkota, A.R. (2017) Antibiotic Concentrations Decrease during Wastewater Treatment but Persist at Low Levels in Reclaimed Water, *Int J Environ Res Public Health* **14**: 668.

Le, T.H., Ng, C., Tran, N.H., Chen, H., and Gin, K.Y.H. (2018) Removal of antibiotic residues, antibiotic resistant bacteria and antibiotic resistance genes in municipal wastewater by membrane bioreactor systems, *Water Research* **145**: 498-508.

Lean, S.S., and Yeo, C.C. (2017) Small, Enigmatic Plasmids of the Nosocomial Pathogen, Acinetobacter baumannii: Good, Bad, Who Knows?, *Frontiers in Microbiology* **8**: 1547.

Li, B., Qiu, Y., Li, J., Liang, P., and Huang, X. (2019) Removal of antibiotic resistance genes in four full-scale membrane bioreactors, *Sci Total Environ* **653**: 112-119.

Li, Y.H., Lau, P.C., Lee, J.H., Ellen, R.P., and Cvitkovitch, D.G. (2001) Natural genetic transformation of Streptococcus mutans growing in biofilms, *J Bacteriol* **183**: 897-908.

Ma, Y., Wilson, C.A., Novak, J.T., Riffat, R., Aynur, S., Murthy, S., and Pruden, A. (2011) Effect of Various Sludge Digestion Conditions on Sulfonamide, Macrolide, and Tetracycline Resistance Genes and Class I Integrons, *Environmental Science & Technology* **45**: 7855-7861.

Mao, D., Luo, Y., Mathieu, J., Wang, Q., Feng, L., Mu, Q., et al. (2014) Persistence of extracellular DNA in river sediment facilitates antibiotic resistance gene propagation, *Environmental Science and Technology* **48**: 71-78.

McConnell, M.M., Truelstrup Hansen, L., Jamieson, R.C., Neudorf, K.D., Yost, C.K., and Tong, A. (2018) Removal of antibiotic resistance genes in two tertiary level municipal wastewater treatment plants, *Sci Total Environ* **643**: 292-300.

Michael, I., Rizzo, L., McArdell, C.S., Manaia, C.M., Merlin, C., Schwartz, T., et al. (2013) Urban wastewater treatment plants as hotspots for the release of antibiotics in the environment: A review. *Water Research*. 957-995.

Munir, M., Wong, K., and Xagoraraki, I. (2011) Release of antibiotic resistant bacteria and genes in the effluent and biosolids of five wastewater utilities in Michigan, *Water research* **45**: 681-693.

Nielsen, K.M., Johnsen, P.J., Bensasson, D., and Daffonchio, D. (2007) Release and persistence of extracellular DNA in the environment, *Environmental Biosafety Research* **6**: 37-53.

Okshevsky, M., and Meyer, R.L. (2015) The role of extracellular DNA in the establishment, maintenance and perpetuation of bacterial biofilms, *Crit Rev Microbiol* **41**: 341-352.

O'Neil, J. (2014) AMR Review Paper - Tackling a crisis for the health and wealth of nations.

Pei, R., Kim, S.C., Carlson, K.H., and Pruden, A. (2006) Effect of river landscape on the sediment concentrations of antibiotics and corresponding antibiotic resistance genes (ARG), *Water Res* **40**: 2427-2435.

Phuong Hoa, P.T., Nonaka, L., Hung Viet, P., and Suzuki, S. (2008) Detection of the sul1, sul2, and sul3 genes in sulfonamide-resistant bacteria from wastewater and shrimp ponds of north Vietnam, *Sci Total Environ* **405**: 377-384.

Pruden, A., Larsson, D.G.J., Amézquita, A., Collignon, P., Brandt, K.K., Graham, D.W., et al. (2013) Management options for reducing the release of antibiotics and antibiotic resistance genes to the environment, *Environmental health perspectives* **121**: 878-885.

Pruden, A., Pei, R., Storteboom, H., and Carlson, K.H. (2006) Antibiotic Resistance Genes as Emerging Contaminants: Studies in Northern Colorado, *Environmental Science & Technology* **40**: 7445-7450.

Prudhomme, M., Attaiech, L., Sanchez, G., Martin, B., and Claverys, J.-P. (2006) Antibiotic Stress Induces Genetic Transformability in the Human Pathogen *Streptococcus pneumoniae*, *Science* **313**: 89.

Quach-Cu, J., Herrera-Lynch, B., Marciniak, C., Adams, S., Simmerman, A., and Reinke, A.R. (2018) The Effect of Primary, Secondary, and Tertiary Wastewater Treatment Processes on Antibiotic Resistance Gene (ARG) Concentrations in Solid and Dissolved Wastewater Fractions, *Water* **10**: 37.

Rowe, W., Verner-Jeffreys, D.W., Baker-Austin, C., Ryan, J.J., Maskell, D.J., and Pearce, G.P. (2016) Comparative metagenomics reveals a diverse range of antimicrobial resistance genes in effluents entering a river catchment, *Water Sci Technol* **73**: 1541-1549.

San Millan, A., Escudero, J.A., Gutierrez, B., Hidalgo, L., Garcia, N., Llagostera, M., et al. (2009) Multiresistance in *Pasteurella multocida* is Mediated by Coexistence of Small Plasmids, *Antimicrobial Agents and Chemotherapy* **53**: 3399.

Shintani, M., Sanchez, Z.K., and Kimbara, K. (2015) Genomics of microbial plasmids: classification and identification based on replication and transfer systems and host taxonomy, *Frontiers in microbiology* **6**: 242-242.

Slager, J., Kjos, M., Attaiech, L., and Veening, J.W. (2014) Antibiotic-induced replication stress triggers bacterial competence by increasing gene dosage near the origin, *Cell* **157**: 395-406.

578 Smith, A.L., Skerlos, S.J., and Raskin, L. (2013) Psychrophilic anaerobic membrane
579 bioreactor treatment of domestic wastewater, *Water Research* **47**: 1655-1665.
580 Smith, A.L., Stadler, L.B., Love, N.G., Skerlos, S.J., and Raskin, L. (2012) Perspectives
581 on anaerobic membrane bioreactor treatment of domestic wastewater: a critical review,
582 *Bioresource Technology* **122**: 149-159.
583 Sugimoto, S., Sato, F., Miyakawa, R., Chiba, A., Onodera, S., Hori, S., and Mizunoe, Y.
584 (2018) Broad impact of extracellular DNA on biofilm formation by clinically isolated
585 Methicillin-resistant and -sensitive strains of Staphylococcus aureus, *Scientific Reports* **8**:
586 2254.
587 Wang, D.N., Liu, L., Qiu, Z.G., Shen, Z.Q., Guo, X., Yang, D., et al. (2016) A new
588 adsorption-elution technique for the concentration of aquatic extracellular antibiotic
589 resistance genes from large volumes of water, *Water Res* **92**: 188-198.
590 Watve, M.M., Dahanukar, N., and Watve, M.G. (2010) Sociobiological Control of Plasmid
591 Copy Number in Bacteria, *PLOS ONE* **5**: e9328.
592 Wu, S., Dalsgaard, A., Hammerum, A.M., Porsbo, L.J., and Jensen, L.B. (2010)
593 Prevalence and characterization of plasmids carrying sulfonamide resistance genes
594 among Escherichia coli from pigs, pig carcasses and human, *Acta veterinaria*
595 *Scandinavica* **52**: 47-47.
596 Wu, S., Dalsgaard, A., Hammerum, A.M., Porsbo, L.J., and Jensen, L.B. (2010)
597 Prevalence and characterization of plasmids carrying sulfonamide resistance genes
598 among Escherichia coli from pigs, pig carcasses and human, *Acta Vet Scand* **52**: 47.
599 Xiong, Y., Harb, M., and Hong, P.Y. (2017) Performance and microbial community
600 variations of anaerobic digesters under increasing tetracycline concentrations, *Applied*
601 *Microbial Biotechnology* **101**: 5505-5517.
602 Xu, Y., Guo, C., Luo, Y., Lv, J., Zhang, Y., Lin, H., et al. (2016) Occurrence and distribution
603 of antibiotics, antibiotic resistance genes in the urban rivers in Beijing, China,
604 *Environmental Pollution* **213**: 833-840.
605 Zafra, O., Lamprecht-Grandío, M., de Figueras, C.G., and González-Pastor, J.E. (2012)
606 Extracellular DNA Release by Undomesticated Bacillus subtilis Is Regulated by Early
607 Competence, *PLOS ONE* **7**: e48716.
608 Zarei-Baygi, A., Harb, M., Wang, P., Stadler, L.B., and Smith, A.L. (2019) Evaluating
609 Antibiotic Resistance Gene Correlations with Antibiotic Exposure Conditions in Anaerobic
610 Membrane Bioreactors, *Environmental Science & Technology* **53**: 3599-3609.
611 Zhang, Y., Li, A., Dai, T., Li, F., Xie, H., Chen, L., and Wen, D. (2018) Cell-free DNA: A
612 Neglected Source for Antibiotic Resistance Genes Spreading from WWTPs,
613 *Environmental Science and Technology* **52**: 248-257.
614 Zheng, J., Su, C., Zhou, J., Xu, L., Qian, Y., and Chen, H. (2017) Effects and mechanisms
615 of ultraviolet, chlorination, and ozone disinfection on antibiotic resistance genes in
616 secondary effluents of municipal wastewater treatment plants, *Chemical Engineering*
617 *Journal* **317**: 309-316.
618 Zhu, L., Zhang, Y., Fan, J., Herzberg, M.C., and Kreth, J. (2011) Characterization of
619 competence and biofilm development of a Streptococcus sanguinis endocarditis isolate,
620 *Mol Oral Microbiol* **26**: 117-126.
621

622

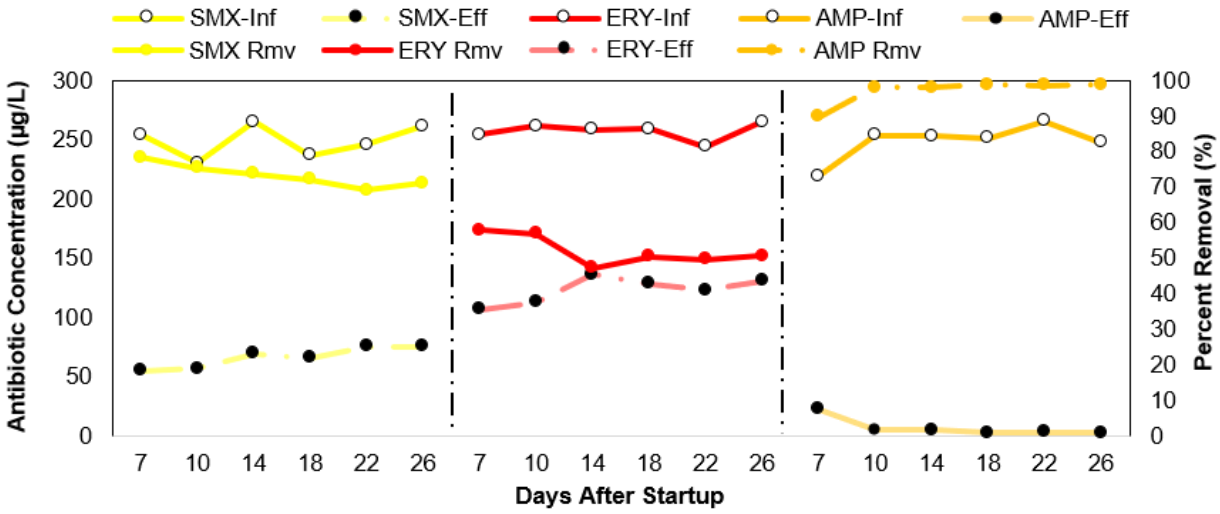

623

624 **Figure 1:** Measured antibiotic concentrations in the influent and effluent of AnMBR along
625 with antibiotic removal percentage. Antibiotics (ampicillin, erythromycin, and
626 sulfamethoxazole) were added to influent at a final concentration of 250 µg/L from day 3
627 to day 35.

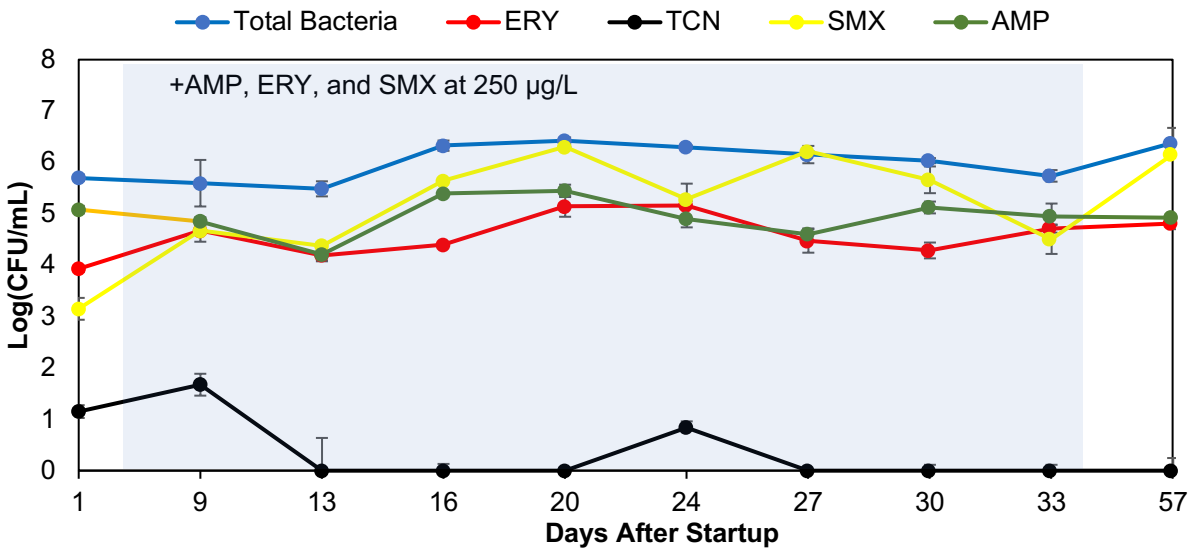

628

629 **Figure 2:** Heterotrophic plate count for effluent total bacteria, erythromycin resistant
630 bacteria (ERY), tetracycline resistance bacteria (TET), sulfamethoxazole resistant

631 bacteria (SMX), and ampicillin resistant bacteria (AMP) over the experimental run. All
632 samples were plated in duplicate. The addition of antibiotics lasted from day 3 to day 35.

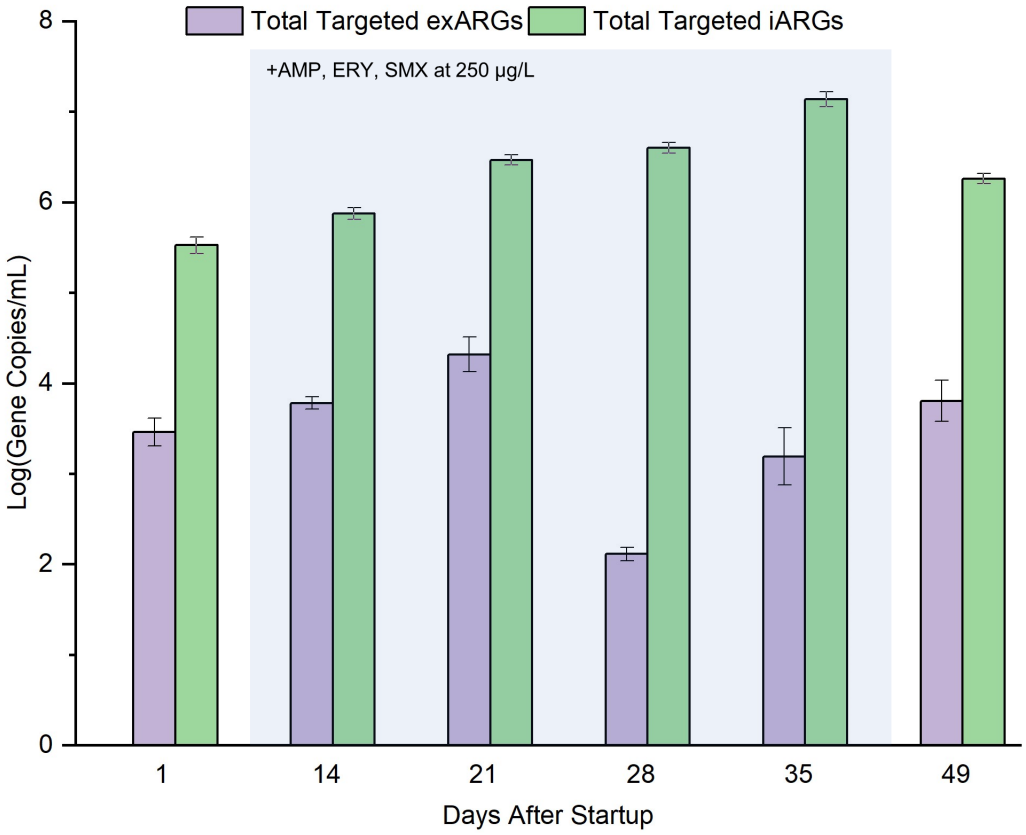

633

634 **Figure 3:** Abundance of total targeted intracellular and extracellular ARGs over the
635 course of the experiment. Targeted ARGs consisting of *amp*C, *erm*F, *sul*1, *sul*2, *tet*W,
636 *tet*O, and *oxa*-1 were summed for each sampling date and plotted as log(Gene
637 Copies/mL). The mixed antibiotics period lasted from day 3 to day 35.

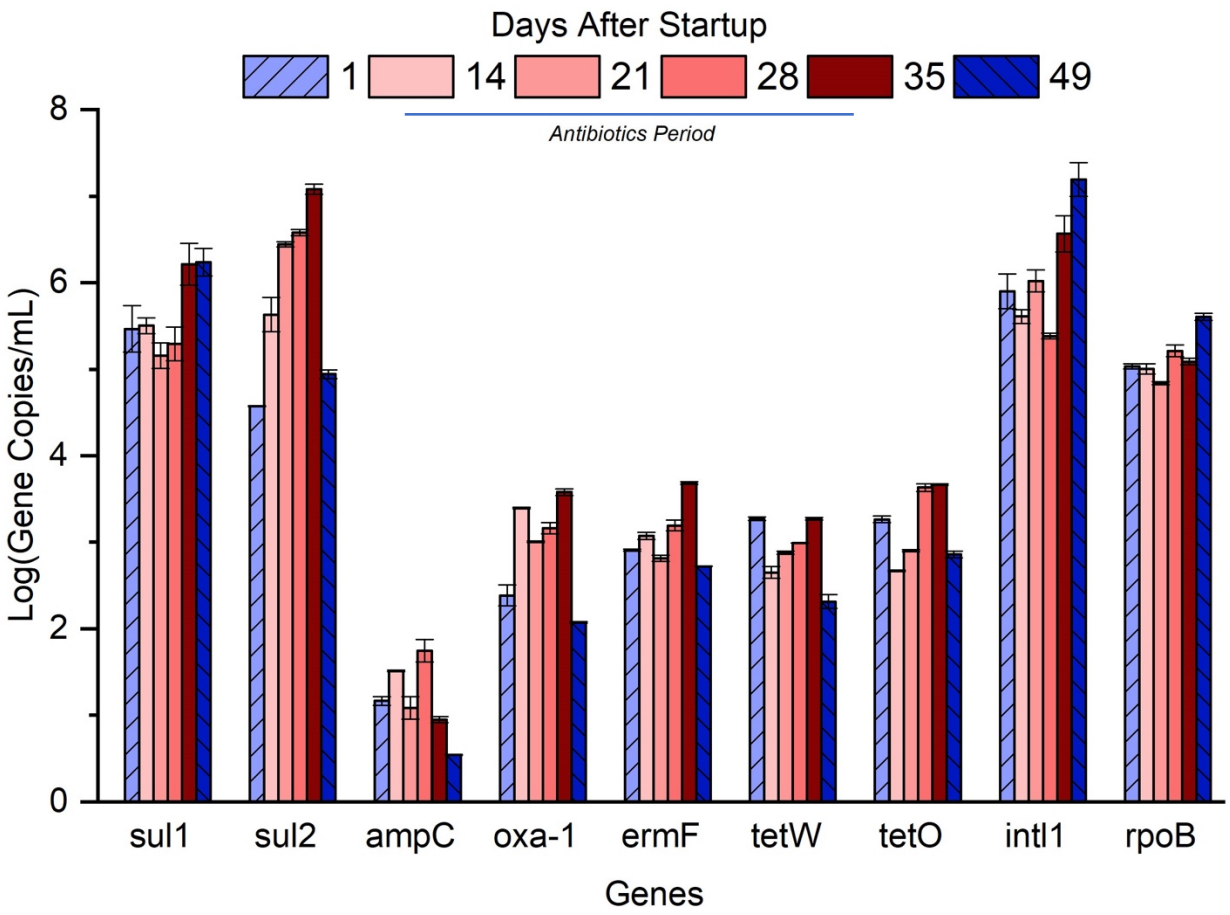

Figure 4: Abundance of targeted intracellular ARGs, *int*I1, and *rpo*B (Gene Copies/mL) in the AnMBR effluent. Error bars represent the mean value and standard deviations of triplicate qPCR runs for each sample. Antibiotics (ampicillin, erythromycin, and sulfamethoxazole) were added to influent at a final concentration of 250 µg/L from day 3 to day 35.

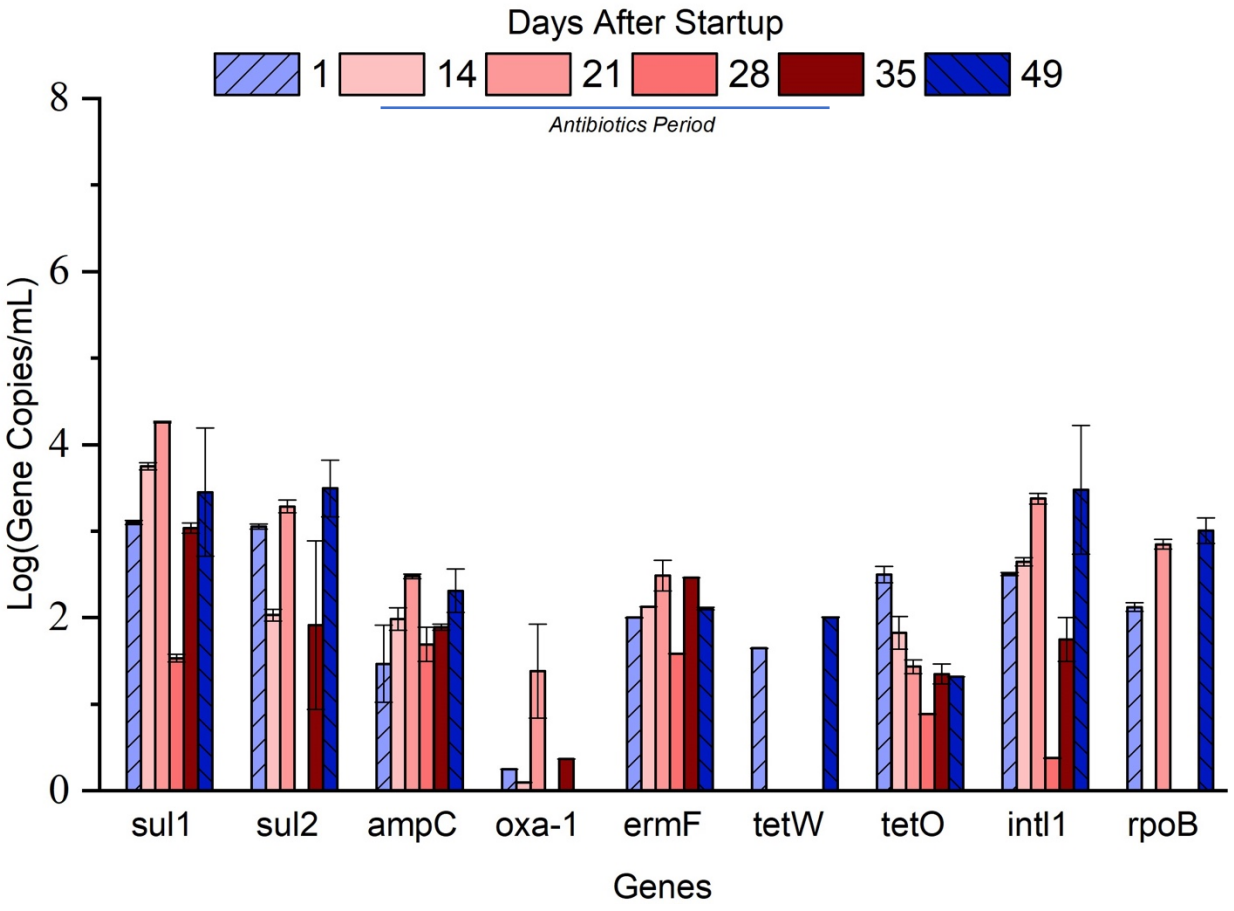

Figure 5: Abundance of targeted extracellular ARGs, *intI*1, and *rpo*B log(Gene Copies/mL) in the AnMBR effluent during the course of the experimental run. Error bars represent the mean value and standard deviations of triplicate qPCR runs for each sample. Antibiotics (ampicillin, erythromycin, and sulfamethoxazole) were added to influent at a final concentration of 250 µg/L from day 3 to day 35. Detection limit for each ARG are provided in (SI Table 2)

Supporting Information

Comparative analysis of intracellular and extracellular antibiotic resistance gene abundance in anaerobic membrane bioreactor effluent

Phillip Wang*, Moustapha Harb*, Ali Zarei-Baygi*, Lauren B. Stadler, and Adam L. Smith*†**

*Astani Department of Civil and Environmental Engineering, University of Southern California, 3620 S V*erm*ont Ave, Los Angeles, CA 90089, USA
** Department of Civil and Environmental Engineering, Rice University, 6100 Main Street, Houston, TX 77005, USA

†Corresponding author (Adam L. Smith)
Phone: +1 213.740.0473
Email: smithada@usc.edu

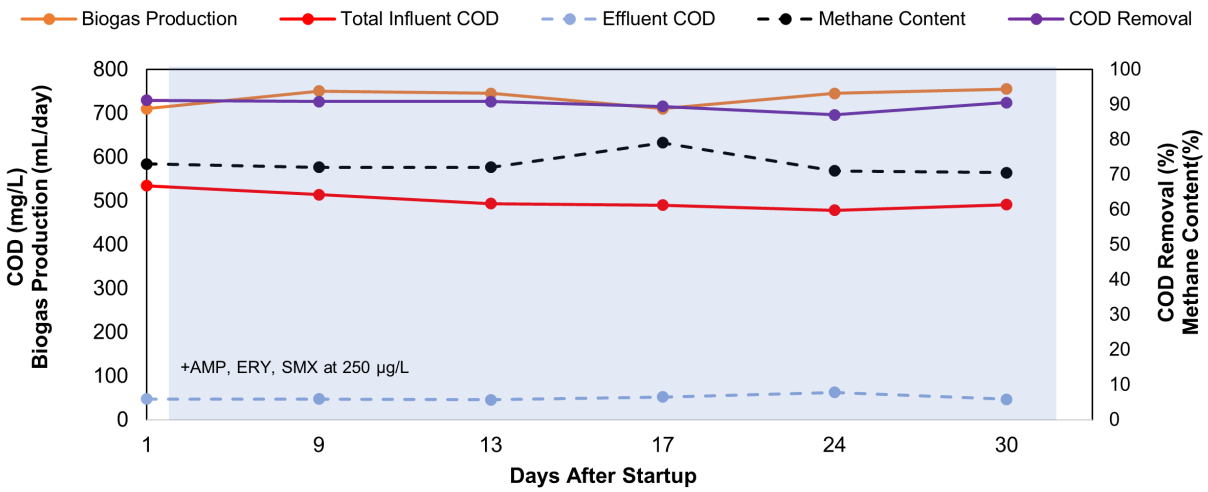

690

691 **SI Figure 1:** AnMBR performance for COD removal and biogas production during the
692 addition of antibiotics. Biogas production, total COD and effluent COD concentrations are
693 plotted on the primary y-axis. COD removal and methane content are plotted on the
694 secondary y-axis. Antibiotics (ampicillin, erythromycin, and sulfamethoxazole) were
695 added to influent at a final concentration of 250 µg/L from day 3 to day 35.

696
697
698
699
700
701
702
703
704
705
706

Bench-scale anaerobic membrane bioreactor operation

The bench-scale AnMBR contained 5 liters of sludge with a MLSS and MLVSS 7.9±0.4 g/L and 6.1 ± 0.5 g/L, respectively. The influent consisted of synthetic wastewater, which was prepared twice a week. The synthetic wastewater contains two components. A concentration solution and a dilution water. The concentrate solution and dilution water were combined at a ratio of 1:9 to achieve the final concentration for the feed. Table S1 lists the components and final concentration for both solutions.

Concentrate solution		Dilution water	
Composition	Concentration (mg/L)	Composition	Concentration (mg/L)
Ammonium Chloride	11.5	Sodium Bicarbonate	369
Calcium Chloride	11.5	Magnesium Phosphate	30.8
Iron Sulfate	7.7	Potassium Phosphate	13.8
Sodium Sulfate	11.5	Sodium hydroxide	18.5
Sodium Acetate	27		
Urea	87		
Peptone	11.5		
Yeast	46		
Milk Powder	115.4		
Soy Oil	13.5		
Hydrochloric acid	0.2		
Starch	115.4		
Chromium Nitrate	3.7		
Copper Chloride	2.5		
Manganese Sulfate	4.9		
Nickel Sulfate	1.2		
Lead Chloride	0.5		
Zinc Chloride	1.2		

SI Table S1: Synthetic wastewater composition

Membrane modules were physically cleaned and submerged in 0.5% (v/v) NaOCl solution overnight. In addition, a peristaltic pump was used to continuously circulate the 0.5% NaOCl solution through the membranes. To return the permeate back to neutral pH, the membrane modules were pumped with DI water for 3 hours. During the DI water

720 pumping period, the permeate flux and transmembrane pressure (TMP) results did not
721 indicate any signs of irreversible fouling throughout the experimental run.

722 A flowmeter (GFM17 Flow Meter, Aalborg, Orangeburg, NY) was used to measure
723 the production of total biogas. The recirculation of headspace biogas through the sparging
724 tubes underneath the membrane modules (rate = 30 ml/min) served to scour the surface
725 of the membranes and prevent membrane fouling. The working volume of the reactor was
726 maintained using an automatic level float switch. Effluent permeate flow was controlled
727 at a rate of 8 min filtration and 2 min backwashing per 10 min period using a peristaltic
728 pump (BT100-1L Multi-channel Peristaltic Pump, Longer, China). Pressure transducers
729 measured the TMP of each membrane module. The permeate flux was set at 7 LMH,
730 which led to hydraulic retention time (HRT) of 16 hours. No sludge was wasted except for
731 sampling, which resulted in a solids retention time (SRT) of 300 days. The software
732 LabVIEW 2014 (Student Edition) was used to monitor and record all relevant AnMBR
733 operational parameters.

734 Chemical oxygen demand (COD) was measured in accordance with USEPA
735 Method 410.4 using a HI801 Spectrophotometer (Hanna Instruments, Woonsocket, RI,
736 USA). Volatile fatty acids (acetate, propionate, formate and valerate), sulfate, phosphate
737 and chloride were measured by ion chromatography on an ICS 2100 (Thermo Fisher
738 Scientific, Waltham, MA) using methods described previously (Chen and Smith, 2018).
739 Headspace biogas samples and effluent were analyzed using a Trace 1310 GC system
740 (Thermo Scientific, NY) with flame ionization detection (FID) as described previously
741 (Chen and Smith, 2018).

Gene	Primers	Preincubation	Amplification	Melting	Amplification size (bp)	Detection limit (gene copy/mL)
ermF	F- CGACACAGCTTTGGTTGAAC R- GGACCTACCTCATAGACAAG	95° for 900 s	40 cycles, 95° for 30 s, 56° for 60 s, 70° for 60	95° for 10 s, 65° for 60 s, 97° for 1 s	309	350
sul1	F- CGCACCGGAAACATCGCTGCAC R- TGAAGTTCCGCCGCAAGGCTCG	95° for 300 s	40 cycles, 95° for 15 s, 58° for 30 s, 72° for 30 s	95° for 10 s, 65° for 60 s, 97° for 1 s	163	155
sul2	F- TCCGGTGGAGGCCGGTATCTGG R- CGGGAATGCCATCTGCCTTGAG	95° for 900 s	50 cycles, 95° for 15 s, 58° for 30 s, 72° for 30 s	95° for 10 s, 65° for 60 s, 97° for 1 s	191	821
intl1	F- CTGGATTTCGATCACGGCACG R- ACATGCGTGTAAATCATCGTCG	95° for 900 s	45 cycles, 95° for 30 s, 60° for 60 s	95° for 10 s, 65° for 60 s, 97° for 1 s	196	159
oxa-1	F- TATCTACAGCAGCGCCAGTG R- CGCATCAAATGCCATAAGTG	94° for 180 s	40 cycles, 94° for 30 s, 60° for 30 s, 72° for 60 s	N/A	199	12100
ampC	F- CCTCTTGCTCCACATTTGCT R- ACAACGTTTGCTGTGTGACG	95° for 300 s	45 cycles, 95° for 45 s, 58° for 45 s, 72° for 60 s	95° for 10 s, 65° for 60 s, 97° for 1 s	189	670
tetO	F- ACGGARAGTTTATTGTATACC R- TGGCGTATCTATAATGTTGAC	95° for 600 s	40 cycles, 95° for 15 s, 50° for 30 s, 72° for 30 s	95° for 10 s, 65° for 60 s, 97° for 1 s	171	2010
tetW	F- GAGAGCCTGCTATATGCCAGC R- GGGCGTATCCACAATGTTAAC	94° for 300 s	40 cycles, 94° for 30 s, 64° for 30 s, 72° for 30 s	95° for 10 s, 65° for 60 s, 97° for 1 s	168	1030
rpoB	F- AACATCGGTTTGATCAAC R- CGTTGCATGTTGGTACCCAT	95° for 300 s	40 cycles, 95° for 30 s, 55° for 30 s, 72° for 30 s	95° for 10 s, 65° for 60 s, 97° for 1 s	381	5430
pUC19	M13 Forward (F)- TGTAAAACGACGGCCAGT L4440 (R)- AGCGAGTCAGTGAGCGAG	95° for 300 s	40 cycles, 95° for 30 s, 55° for 30 s, 72° for 30	95° for 10 s, 65° for 60 s, 97° for 1 s	335	550

SI Table S2: qPCR thermocycling conditions for all forward and reverse primers used in this study

Antibiotic quantification

All glassware used for antibiotic quantification were baked at 400 ºC for a at least one hour and washed with methanol prior to use. Influent and effluent samples (10 mL) and standard solutions were filtered using a 0.2 µm PTFE syringe filters (Whatman) and a 10 mL syringe with Luer lock tip. Prepped samples were preserved in certified 2 mL amber LC vials (Agilent) and stored at 4 ºC for no more than 3 days prior to analysis. Stock solutions of SMX and ERY were prepared in HPLC-grade methanol at concentrations of 20 mg/L and stored at -20 ºC. AMP stock solution was prepared in HPLC-grade water at 20 mg/L because of its insolubility in methanol and stored at 4 ºC. Five-point standard calibration curves were generated within the appropriate range for each of the incremental antibiotic influent concentration phases (i.e., 0.1-15 µg/L for 10 µg/L, 0.5-70 µg/L for 50 µg/L, and 1-300 µg/L for 250 µg/L). All calibration curve R^2 values were > 99%. Both solvent-based and matrix-matched calibration curves were generated for all three compounds to ensure solvent based standards were representative of influent and effluent concentrations. Specifically, SMX, AMP, and ERY were dissolved in influent and effluent solutions at concentrations of 0.1, 1, 10, 100, and 1000 µg/L and processed using the same procedure employed to prepare reactor samples described above. Calibration curves of the results were plotted against standard solutions of the same concentrations dissolved in HPLC-grade water. For all three antibiotics, influent and effluent matrices showed equivalent concentrations and scaling at the ranges detected in the HPLC-grade water with R^2 values of > 99.9. %. No isotope-labelled internal standards were used because the samples were collected and then analyzed by direct injection LC-MS on the same (no solid phase extraction required).

768 SMX, ERY and AMP were all targeted using positive ESI MS-Q-TOF mode. The
769 LC gradient program for detection of all three compounds utilized 0.1% formic acid in
770 water as mobile phase A and acetonitrile as mobile phase B as follows: t=0.0 min A=90%
771 B=10%, t=3.0 min A=0% B=100%, t=5.0 min A=0% B=100%, t=5.10 min A=90% B=10%.
772 LC conditions used included a flow rate of 0.4 mL/min, maximum pressure of 600 bar,
773 column temperature of 40 ºC, and autosampler tray temperature of 8 ºC. A post-column
774 switch was used to divert the first 0.5 min of column elution to waste to avoid sending
775 hydrophilic compounds from the effluent matrix through the MS. Injection volumes ranged
776 from 0.5-10 µL, depending on the target sample range for each operational phase, to
777 ensure that no compound extracted ion chromatogram peaks exceeded saturation
778 detection values. MS conditions used were as follows: sheath gas temp. of 400 ºC, sheath
779 gas flow rate of 12 L/min, gas temperature of of 225 ºC, drying gas flow rate of 5 L/min,
780 nebulizer pressure of 20 psi, capillary voltage of 3500V, nozzle voltage of 500V,
781 acquisition rate of 1.5 spectra/s, and acquisition time of 667 ms/spectrum. Targeted
782 compound acquisition parameters are provided in Table S2. All compound detection and
783 quantification analyses were performed using the Agilent MassHunter Qualitative
784 Analysis Navigator program.

785

786

787

Compound	Molecular Weight (MW)	Retention Time (min)	MS Spectrum (m/z)	Fragmentor Voltage (V)
Sulfamethoxazole	253.052	2.17	254.059	400
Erythromycin	733.461	2.35	734.469	100
Ampicillin	349.110	1.44	350.117	400

788

789 **SI Table S3**. Targeted antibiotic properties and MS data acquisition parameters

790

791 **Quantification of ARGs using real time qPCR**

792 All ARG standards used for qPCR quantification were constructed from PCR
793 (Mastercycler nexus, Eppendorf, Hamburg, Germany) amplified products of DNA extracts
794 from activated sludge (listed in Table S2). DNA samples from activated sludge. PCR
795 products were analyzed on 2% agarose gel electrophoresis to verify the correct amplicon
796 size. The correct DNA bands of interest were purified using Wizard® SV Gel and PCR
797 Clean-Up System (Promega, Madison, WI). Purified amplicons were cloned into
798 linearized pMiniT 2.0 vector and transformed into NEB 10-beta Competent *E. coli* using
799 the NEB PCR Cloning Kit (New England Biolabs, Ipswich, MA). Trasnformed E. *coli* were
800 selected for on AMP selection plates. AMP resistant E. coli cells were harvested, and its
801 plasmids was extracted using PureLink™ Quick Plasmid Miniprep kit (Invitrogen,
802 Carlsbad, CA). Plasmid extracts were sent for Sanger sequencing (Laragen Sequencing
803 & Genotyping, Culver City, CA) to confirm the presence of target ARG.. DNA
804 concentration of the plasmid extracts were measured using the Quant-iT PicoGreen
805 dsDNA Assay Kit (Invitrogen, Carlsbad, CA). Standard curves were established using
806 serial dilutions of the purified plasmids (10^{-1} to 10^{-8}). For all ARGs, the *intI*1 gene, and the
807 *rpo*B gene, qPCR efficiencies ranged from 92% to 102%. Melting curve and gel
808 electrophoresis were performed to assure the specificity of each qPCR reaction. SI Table
809 2 shows the forward and reverse primers, annealing temperatures, and thermal cycling
810 conditions of all ARGs, *intI*1 and *rpo*B..

811